

# Study of erosion behaviour of conventional and nanostructured WC-12Co coatings sprayed by atmospheric plasma

V. Bonache<sup>1a</sup>, M.D. Salvador<sup>1b</sup>, J.C. García<sup>1c</sup>, V. García<sup>1d</sup>, E. Sanchez<sup>2e</sup>, M. Vicent<sup>2f</sup>

<sup>1</sup>Instituto de Tecnología de Materiales. Universidad Politécnica de Valencia. Camino de Vera s/n 46022. Valencia (España)

<sup>2</sup>Instituto de Tecnología Cerámica. ITC. Universitat Jaume I. Campus de Riu Sec. 12071. Castellón (España)

<sup>a</sup>vicbobe@doctor.upv.es, <sup>b</sup>dsalva@mcm.upv.es, <sup>c</sup>jcgarr@upvnet.upv.es, <sup>d</sup>mvigardo@euitiv.upv.es, <sup>e</sup>enrique.sanchez@itc.uji.es, <sup>f</sup>monica.vicent@itc.uji.es

**Keywords:** WC-Co coatings, nanostructured powders, plasma spraying, resistant behaviour, erosion resistance.

**Abstract.** Thermal sprayed WC-Co coatings are used extensively to enhance the wear resistance of a wide range of engineering components. In this paper, erosive resistance of plasma atmospheric sprayed WC-12Co coatings has been evaluated. Solid particle erosion tests were conducted on these coatings at different angles of impact with silica and alumina abrasives of size 250  $\mu\text{m}$ . Coatings have been deposited by using micrometric and nanometric agglomerated powders, employing  $\text{H}_2$  and He as plasmogen gas. In order to determine the erosion regime (ductile or brittle), the influence of impact angle on the erosion rate has been studied. Optical microscope and FESEM have been used to analyze the eroded surface. The influence of the plasmogen gas and the powder employed on the erosive behaviour of the coating has been evaluated. An attempt to connect the erosive behaviour with mechanical properties and microstructure has been made. Hardness has been determined by means of several measurements of Vickers microhardness; fracture toughness has been estimated through indentation method. Identification of phases has been made by means of X Ray diffraction.

## 1. Introduction

WC-Co coatings deposited by thermal spraying have been widely used for applications where high wear and erosive resistance is required. These coatings exhibit multi-phase microstructures, being generally formed of WC,  $\text{W}_2\text{C}$ , W and an amorphous binder phase, based on Co [1, 2]. Solid particle erosion is a serious problem for industrial equipment, for example walls of pipelines used for the pneumatic transportation of pulverized coal in power stations. The gas-blast method of erosion testing is widely used in order to evaluate the erosive resistance of many materials. In this method, abrasive particles are accelerated in a gas stream along a nozzle before striking the specimen. Erosion can occur in two different regimes: ductile or brittle. Erosion rate depends on impact angle of abrasive particles. In ductile regime, erosion rate is maximum at an angle less than  $90^\circ$ , whereas in brittle regime the maximum erosion rate is achieved at  $90^\circ$  [3, 4]. Studies by Anand and Conrad [5] in sintered WC-Co materials established that the erosion behavior of WC-Co alloys could be changed from a brittle-type, characterized by maximum erosion at 90 degrees, to a ductile-type with maximum erosion at lower angles, by decreasing the WC grain size or by increasing the erodent particle size and velocity. However in WC-Co coatings, erosion behavior is not as clear and the effect of the microstructure on the erosion resistance is not well known.

The objective of the present paper is to study the erosive behavior of four kinds of plasma sprayed coatings and to investigate the effect of erosive property and impingement angle on the erosive rate of the coatings. Special attention is paid to correlating the erosive resistance to the secondary gas used in the spraying process ( $\text{H}_2$  or He) and to the size of the powder particles sprayed (micrometric or nanometric).

## 2. Experimental

A high power atmospheric plasma spray system has been used. It is comprised of a Sulzer Metco F4-MB gun, moved by an IRB 1400 robot from ABB. The voltage has been kept constant at 62 V and a nozzle of 1.8 mm has been used. The spray conditions are presented in Table 1. Ar has been used as primary plasma gas, whereas H<sub>2</sub> and He have been employed as secondary gas.

Table 1. Parameters employed during Plasma spraying.

Ar (slpm)	H <sub>2</sub> (slpm)	He (slpm)	Intensity (A)	Spraying distance (mm)	Spraying velocity (mm/s)	Mass flow (g/min)
65	3	-	750	130	1000	50
60	-	120	625	110	1000	30

Two kinds of powders have been used, micrometric powder and nanometric powder. The characteristics of the powders are shown in table 2. The granulometric size (table 2) refers to the size of the agglomerates. The nanometric agglomerates are constituted for particles of size ranging from 50 to 500 nm. Fig 1 shows the morphology of the powders and the morphology of the agglomerates prepared for the spraying.

Table 2. Characteristics of the powders employed

Powder	Supplier	Reference	Composition	Granulometric size
Conventional	Sulzer-Metco	72F-NS	WC-12Co	15 a 45 μm
Nanometric	Inframat AM	Infralloy S7412	WC-12Co	5 a 45 μm

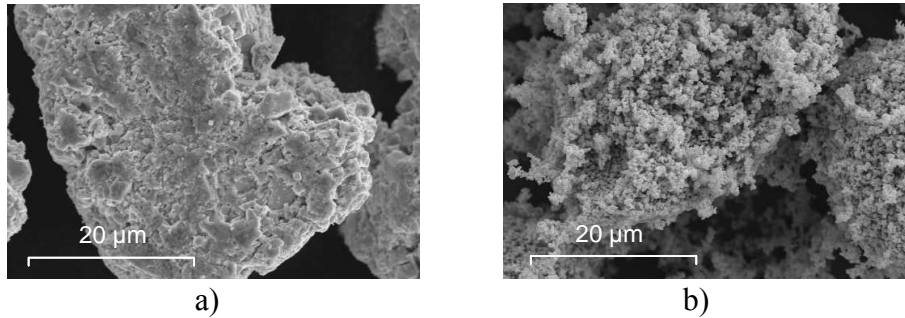


Fig.1. FESEM micrographs of the powders employed: a) micrometric, b) nanometric

The powders have been sprayed on carbon steel substrates. Before spraying, the substrates have been grit-blasted on one side to clean and roughen the surface.

In order to identify the present phases, XRD has been performed on the surface of the coatings. The porosity has been measured by means of image analysis of the optical micrographs. The microhardness tests have been performed using Matsuzawa MHT2 micro-hardness tester at 500 g load and a dwell time of 15 s. Fracture toughness ( $K_{IC}$ ) has been estimated by Vickers indentation technique at 1 kg load. Lawn and Fuller equation has been employed to calculate toughness [6].

$$K_{IC} = 0.0515 \frac{P}{c^{3/2}} \quad (1)$$

Where P is the load applied (N); c is crack length measured from the centre of the indentation (m).

The erosion tests were carried out with a gas blasting apparatus. The nozzle has an internal diameter of 3 mm and the specimen is placed at a distance of 15 mm from the nozzle. Before and after an erosion test, the specimen has been cleaned by means of compressed air, brushing and keeping it in ultrasounds for 15 minutes. The mass loss was determined by weighting the samples before and after the test using an electronic precision balance with an accuracy of  $\pm 0.1$  mg. The erosion rate ( $\epsilon$ ) was determined by the following equation:

$$\varepsilon = \frac{m}{M} \quad (2)$$

Where  $m$  (g) represents the mass lost by the sample during the erosion test and  $M$  (g) is the mass of erodent that have impacted the sample. The erodents used have been  $\text{Al}_2\text{O}_3$  and  $\text{SiO}_2$ . Eroder particles have approximately a size of  $250 \mu\text{m}$  and their morphology can be observed in FESEM images shown in figure 2.

FESEM have also been used to analyze the erodent surface and to study erosion mechanisms.

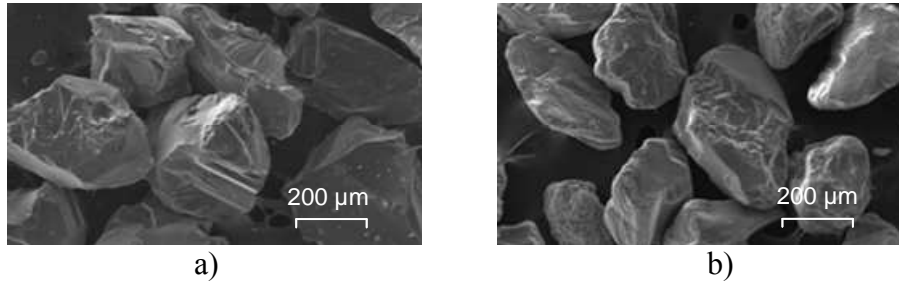


Fig. 2. FESEM micrographs of erodents: a)  $\text{Al}_2\text{O}_3$ , b)  $\text{SiO}_2$

### 3. Results.

As it can be seen in Fig.3, the coatings are constituted by three crystalline phases (WC,  $\text{W}_2\text{C}$  and W). WC is present in the initial powder but the other two phases have been formed during the spraying process through the decarburization of the WC particles. XRD analysis also revealed that the proportion of secondary phases ( $\text{W}_2\text{C}$  and W) is higher in the coatings sprayed using  $\text{H}_2$  as shown Fig. 3 (the  $\text{W}_2\text{C}$  and W peaks are higher). The plasma created employing  $\text{H}_2$  is more energetic and therefore the decarburization of the WC particles in the gas jet is higher.

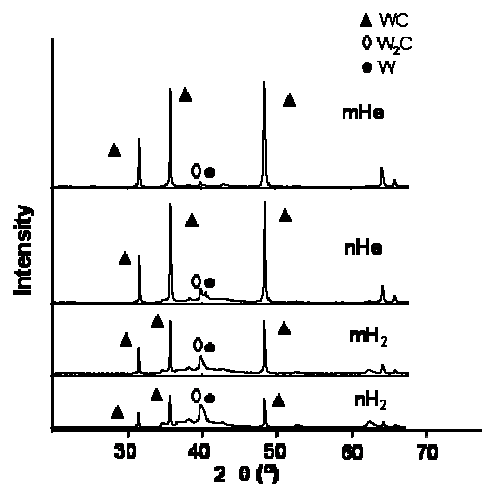


Fig. 3. XRD scans for coatings sprayed using micrometric powder and  $\text{H}_2$  ( $\text{mH}_2$ ), micrometric powder and He ( $\text{mHe}$ ), nanometric powder and  $\text{H}_2$  ( $\text{nH}_2$ ), nanometric powder and He ( $\text{nHe}$ ).

The porosity obtained is about 10% and the thickness is approximately  $200 \mu\text{m}$ , as can be seen en Fig. 4b. The presence of WC and the secondary phases (W and  $\text{W}_2\text{C}$ ) previously detected by XRD has been confirmed by means of FESEM. Observations of coatings using backscattered electron (BSE) imaging has allowed to identify the presence of a matrix phase which seems to be Co-rich. This Co-rich phase presents areas with different composition. The bright areas belong to matrix areas with high proportion of W (element with the higher mean atomic number). The WC grains are

located inside the “splats”, where the temperature achieved is not high enough to produce the dissolution of the grains.  $W_2C$  has been indentified around the WC grains. W has been detected in the external part of the “splats” where the decarburization grade is higher. It has been demonstrated that it exists more Co-rich matrix in the coatings sprayed using  $H_2$  and nanometric powder. It has also been observed that in the nanometric coatings the WC grains present smaller grains. Fig. 4a shows a SEM image of the coating where are indicated the phases detected by XRD and the areas of Co-rich matrix.

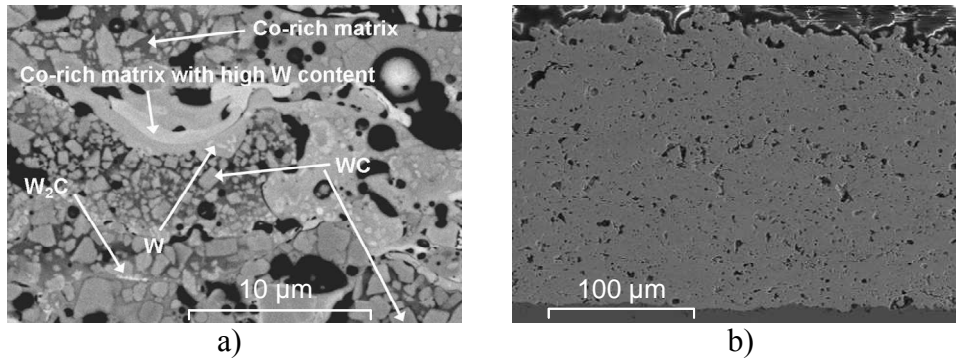


Fig 4. FESEM micrographs of mHe: a) high magnification, b) low magnification

Fig. 5 shows the values of Vickers microhardness and toughness obtained for each coating. It can be seen that the higher microhardness is achieved with the nanometric coatings. The reason of that could be the existence of a higher proportion of  $W_2C$  (phase harder than WC), a higher hardenement of the Co matrix by W dissolution and a smaller WC grain size. The gas used also has a large effect on the values of microhardness obtained. If He is employed, higher values of microhardness are achieved since coatings sprayed using He present a microstructure with more WC grains. Due to the plasma created with He is less energetic, WC decomposition is lower and therefore it is possible to retain a high number of WC grains in the microstructure of the coating. An increase in microhardness is expected when the proportion of WC grains in the microstructure of the coating is higher. It can be seen that the highest values of toughness are achieved when He has been used. These values are similar to the values obtained in the coatings sprayed by HVOF [7]. If  $H_2$  is used, more areas where the WC grains have been completely dissolved in the Co matrix exist. These areas are more brittle and therefore cracks are allowed to propagate more easily.

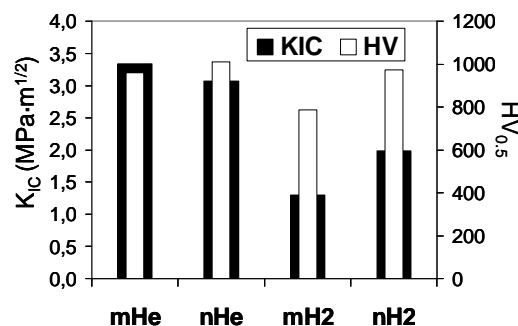


Fig. 5. Vickers microhardness and toughness values obtained for the coatings tested.

Fig. 6. illustrates the relationship between erosion rate and impact angle for each WC-Co coating using alumina and silica erosive particles. The erosion rates are higher when alumina is used but the tendency is similar in both cases. The erosion rate of coatings eroded with alumina is higher due to the higher hardness of alumina, the effect of erodent hardness has been studied in the literature [3]. Moreover, alumina has more cusplate particles that can cause higher erosion rate, which is mainly because these particles can cut and plough the coatings easily [8].

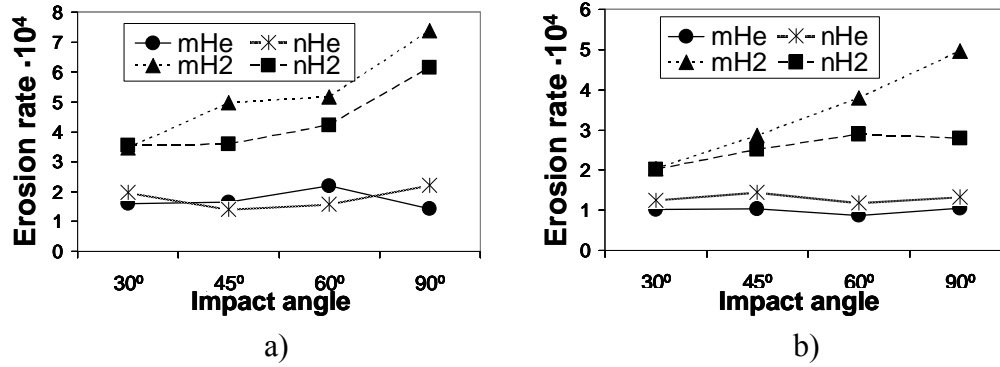


Fig. 6. Effect of impact angle on the erosion rates of coatings using: a)  $\text{Al}_2\text{O}_3$  b)  $\text{SiO}_2$

There is a clear difference between coatings sprayed employing  $\text{H}_2$  and coatings sprayed using He. The values of erosion rate for the coatings deposited with  $\text{H}_2$  are significantly higher than the values obtained using He for both erodents and for all the impact angles. There are not significant differences between the two powders used. Impact angle has a large effect on the erosion rate of coatings sprayed using  $\text{H}_2$  but the influence in coatings sprayed with He is not as clear. In the literature has been proved that in brittle materials the maximum erosion rate occurred at 90° and decreased as the angle of impact was made more oblique [3, 8 and 9]. Coatings sprayed with  $\text{H}_2$  show this tendency and therefore they should be more brittle. The values of toughness obtained correlate perfectly with the erosion results, since, as can be seen in Fig. 5 coatings sprayed with  $\text{H}_2$  present the lowest toughness values and therefore are the most brittle coatings. In Fig. 7 is plotted the erosion rate at 90° and 30° against fracture toughness for the two erodents tested.

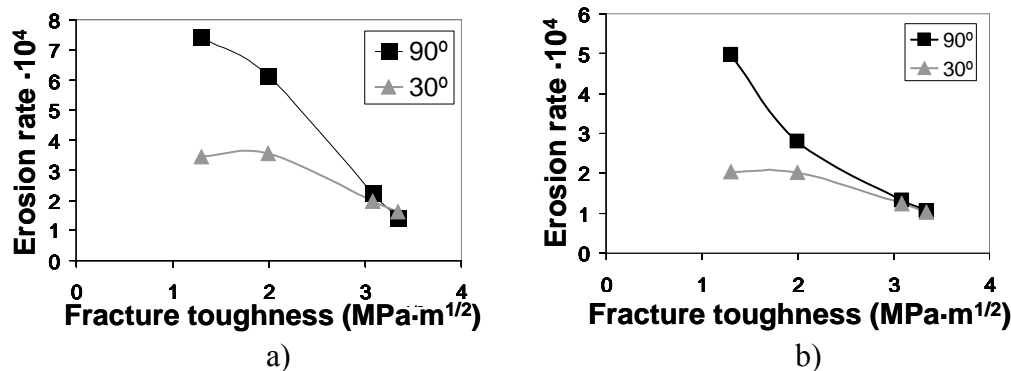


Fig. 7. Variation of erosion rate at 90° and 30° using: a)  $\text{Al}_2\text{O}_3$  b)  $\text{SiO}_2$

It can be seen a definitive tendency for erosion rate to decrease with increasing fracture toughness for all the coatings tested. However the fracture toughness has a higher effect on the erosion rate at 90°. Fig. 8 shows FEM micrographs of eroded surfaces of micrometric coatings sprayed using  $\text{H}_2$  (mH<sub>2</sub>) and He (mHe) at 90°. Due to mH<sub>2</sub> coating presents the lowest value of toughness and mHe coating the highest value, the micrographs of these two coatings have been selected. At 90° the erosion rate of mH<sub>2</sub> coating is approximately 5 times the erosion rate of mHe coating therefore it is expected different mechanisms of erosion. As can be seen in Fig. 8, the mode of erosion for mH<sub>2</sub> coatings is associated with the formation and interaction of cracks in the Co-rich matrix. The Co-rich matrix is brittle and allows that cracks propagate easily. However in mHe coatings the erosion take place mainly by plastic deformation of the binder phase (Co-rich matrix), although some cracks can be found too. Due to the less dissolution of WC in the Co-rich matrix of mHe coatings, the matrix is tougher and therefore it can deform plastically in place of cracking. Moreover mHe coatings have more WC areas that make the cracks propagation difficult. At angles lower than 90° the formation of cracks in mH<sub>2</sub> coating is not as easy and therefore plastic deformation of the binder phase begins to be the main erosion mechanism too. That is the reason why the values of erosion

rate between coatings sprayed with H<sub>2</sub> and coatings sprayed with He are more similar at angles lower than 90°.

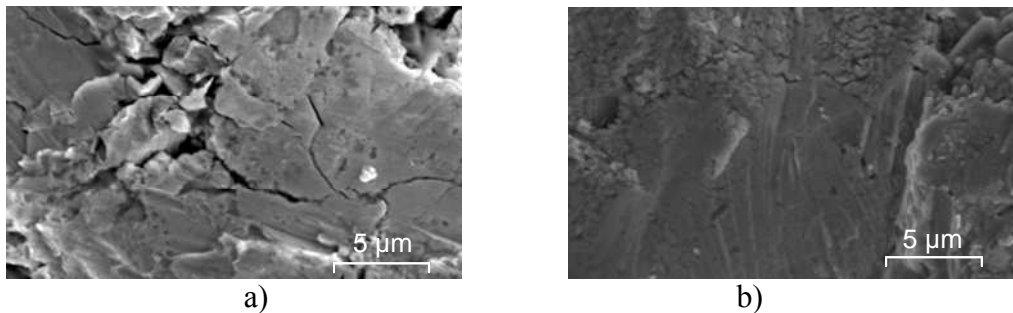


Fig 8. FESEM images of the eroded surfaces at 90° using Al<sub>2</sub>O<sub>3</sub>: a) mH<sub>2</sub> coating, b) mHe coating

#### 4. Conclusions.

- The use of He in the plasma spraying reduces the WC decarburization and dissolution and therefore coatings present higher values of toughness and microhardness.
- The toughness of plasma sprayed WC-Co coatings play an important role in the erosion behaviour. The higher the values of toughness the higher the erosion resistance of the coating.
- The highest erosion rates are achieved by employing Al<sub>2</sub>O<sub>3</sub> erodent due to its higher hardness and its angular morphology.
- Coatings obtained employing He present lower erosion rates for the two erodents used and for all the impact angles tested. At 90° the erosion rate of coatings sprayed with H<sub>2</sub> is approximately 5 times the erosion rate of coatings sprayed with He due to a different erosion mechanism.
- Impact angle has a large effect on the erosion rate of coatings sprayed using H<sub>2</sub> but the influence in coatings sprayed with He is not as clear.
- At lower impact angles the erosion rates between coatings sprayed with He and with H<sub>2</sub> are more similar. This is due to the fact that the main erosion mechanism is the plastic deformation of the binder.

#### Acknowledgements.

The work is supported financially by Ministerio de Educación y Ciencia by means of the project MAT 2006-12945-C03-C02/C01.

#### References

- [1] C. J. Li, A. Ohmori, and Y. Harada, *J. Mater. Sci.*, 31, 785 (1996).
- [2] C. Verdon, A. Karimi, and J.L. Martin, *Mater. Sci Engng A*, 246, 11 (1998).
- [3] R.G. Wellman, and C. Allen, *Wear* 186-187, 117-122 (1995).
- [4] M. Hutchings, *Erosion of ceramic materials*, *Trans Tech*, 75-92 (1992).
- [5] K. Anand and H. Conrad, *Proc. 3rd Int. Conf. Science of Hard Materials*, Nov. 8-13 (1987).
- [6] H. R. Lawn and E.R. Fuller, *J. Mater. Sci.*, Vol. 10, 2014-2016 (1975).
- [7] Sh. Khameneh Asl and M. Heydarzadeh Sohi. *Wear*, 260, 1203-1208 (2006).
- [8] J. Guo, X. Bin-shi, W. Hai-dou, Y. Liang, L. Qing-fen, W. Shi-cheng and C. Xiufang. *Applied Surface Science* 254, 5470-5474 (2008).
- [9] Z. Feng and A. Ball. *Wear* 233-235, 674-684 (1999).